



Science

ELECTRONIC, STRUCTURAL AND PHARMACOKINETIC CHARACTERIZATION OF TRICYCLIC ALKALOID ALTERNAMIDE A: A SEMI-EMPIRICAL QUANTUM STUDY AND ADMET

Sandy Pereira Estácio¹, Francisco Rogênio Da Silva Mendes¹, Emanuelle Machado Marinho², Othon Souto Campos³, Márcia Machado Marinho², Emmanuel Silva Marinho^{*1}

¹ Chemistry Department, State University of Ceará, Brazil

² Chemistry Department, Federal University of Ceará, Brazil

³ Chemistry Department, Federal University of Espírito Santo, Brazil



Abstract

Chagas disease is one of the biggest socioeconomic problems in Latin America. Caused by the protozoan parasite *Trypanosoma cruzi*, affecting 7 million people, causing approximately 14,000 deaths per year. Alternamide, a tricyclic alkaloid present in *Alternanthera littoralis*, an herbaceous plant found on beaches of the Brazilian its extracts are used in traditional medicine for treatment of infectious and inflammatory diseases, which showed anti Trypanocida activity. In this context, in the present work we present the results of the electronic, structural and pharmacokinetic characterization study of the promising phytopharmaceutical Alternamide A. Using the semi-empirical quantum formalism it was possible to identify the most stable conformation, boundary orbitals, calculate to identify nucleophilic sites and reactivity descriptors. Through in silico absorption, distribution, metabolism, excretion and toxicity (ADMET) simulations, including solubility, blood-brain barrier (BBB), plasma protein binding, CYP2D6 binding, gastrointestinal absorption and hepatotoxicity, it was observed that good oral bioavailability and high-water solubility high gastrointestinal absorption. The synthetic accessibility score was 2.75, which means that it would be easy to synthesize the molecule under study. Highlighting what this study represents is a key step for future molecular docking and drug design studies for the development of inhibitors of the evolutionary forms of the molecule T-crossed.

Keywords: Alkaloid; Chagas disease; Neglected disease; Quantum study; Semi-empirical; *Trypanosoma cruzi*.

Cite This Article: Sandy Pereira Estácio, Francisco Rogênio Da Silva Mendes, Emanuelle Machado Marinho, Othon Souto Campos, Márcia Machado Marinho, and Emmanuel Silva Marinho. (2019). "ELECTRONIC, STRUCTURAL AND PHARMACOKINETIC CHARACTERIZATION OF TRICYCLIC ALKALOID ALTERNAMIDE A: A SEMI-EMPIRICAL QUANTUM STUDY AND ADMET." *International Journal of Research - Granthaalayah*, 7(10), 429-447. <https://doi.org/10.29121/granthaalayah.v7.i10.2019.417>.

1. Introduction

Discovered in 1909 by Brazilian doctor Carlos Chagas, Chagas disease is one of the biggest socioeconomic problems in Latin America. It is a zoonosis that affects about 7 million people, which causes approximately 14,000 deaths per year [1]. The causative agent of Chagas disease is *Trypanosoma cruzi*, a flagellated protozoan that in its evolutionary cycle must pass through its hosts of various classes of mammals, including man or even some insects that are known as barbeiro and so the large numbers of infections occurrence [2][3]. It is also one of the neglected diseases, so this pathology does not arouse much interest in the pharmaceutical industries due to the low financial return. Chagas disease chemotherapy is restricted to only two nitroheterocycle drugs, nifurtimox and benznidazole. Therefore, it is of great importance, given the severity and scope of the pathology, to strengthen the research for new trypanocidal agent candidates in their treatment.[4] [5][6][7].

Alternamide A (7,8-dihydroxy-1,2,4,5-tetrahydro-3H-1,5-ethano [c] azepin-3-one), a tricyclic alkaloid isolated from the *Alternanthera littoralis* P. Beauvis, a herbaceous plant commonly found on beaches of the Brazilian eastern coast and its extracts are used in traditional medicine for treatment of infectious and inflammatory diseases, which presented antiprotozoal activity was assayed against trypomastigote forms of *Trypanosoma cruzi* and amastigotes of *Leishmania amazonenses*[8].

Through molecular modeling, we can determine parameters that relate structure and activity [9]. For this, molecular modeling is used, which can be defined as a software system and tools that allow the construction, editing, visualization and analysis of molecular structures. Thus, the computational chemistry allows the complete characterization of the compounds, generating structures with high fidelity rate to native structures and stable conformational geometry, as well as some relevant indices for drug planning. Such as: formation heat, minimum potential energy, homo and lomo energies, dipole moment and the specific arrangement of each atom in the molecule [10] [11] [12]. In addition to electronic and structural characterization, computer modeling allows through models to simulate the behavior of substances in various media, especially with respect to absorption, distribution, metabolism, excretion and toxicity (ADMET) in the human body. The use of algorithms for ADMET simulation are highlighting the discovery and design of new drugs, being applied at an early stage in the research process, promoting both financial and ethical aspects, as well as reducing the initial laboratory cost and use of animals in the development of new medicines [13] [14] [15].

In this context, in the present work, we present the results of the electronic, structural and pharmacokinetic characterization study of the promising phytopharmaco Alternamide A, with initial support for future molecular docking and drug design studies for the development of inhibitors of *T-cruzi* evolutionary forms.

2. Materials and Methods

Computational Details

All the computations were performed on Dell Inspiron personal computer with intel® Core TM i7-4510U processor, 16 GB RAM, 2GB AMD Radeon® video card and Microsoft Windows 8.1® as operating system. All codes used are free license for academic use.

Structural Optimization

Geometry optimization is a technique that aims to find a set of coordinates that minimize the potential energy of the system under study [16]. The basic procedure is to move over the potential surface in the direction in which the energy decreases so that the system is brought to a near local minimum energy. Power minimization makes use of only a small portion of the configuration space. But by adjusting atomic positions, it relaxes distortions in chemical bonds, bond angles, bond lengths, and torsion angles [16][17].

The study of the Alternamide A molecule was carried out using MarvinSket© [18] and ArgusLab® Version 4.0[19] configured to perform semi-empirical calculations (based on the theory of quantum mechanics with Hamiltonian PM3 (Parametric Method 3)[20] , removing some of its molecular characteristics, the Avogadro [21] program was also used to determine the properties of atoms, properties of bonds, angle properties and torsional properties of atoms[22][23][24].

Frontier Orbitals, MESP And Descriptors Reactivity

Electrostatic potential surface maps (MESP) are generated after the overlap in the molecule of a positively charged particle that travels over the van der Waals contact surface and by revealing a repulsion region, represents the positive, white-colored potential, and a region of attraction represents the negative potential of red color, based on equation 1[25][26].

$$V(r) = \sum_A \frac{Z_A}{|\vec{R}_A - \vec{r}|} - \int \frac{\rho(\vec{r}')}{|\vec{r} - \vec{r}'|} d\vec{r}' \quad (1)$$

Since Z is the charge of nucleus A, located at R, A $\rho_A(R)$ is the electron density function for the molecule. V (r) is the resulting electrostatic liquid effect produced at the r point by both electrons and nuclei of the molecule. Since the first term represents the contributions as a function of electron potential and the second term as a function of the nuclei[25].

Using the formalism of molecular orbital theory, we can learn from the LCAO-MO model [9][26], where the orbitals of each molecule are described as linear combinations of the atomic orbitals of the molecule, we can generate the HOMO and LUMO boundary orbitals (respectively , highest occupied orbital molecular and lowest unoccupied molecular orbital), which may indicate the main electron donation and reception sites, respectively. That is, the number of molecular orbitals formed will always be equal to the number of atomic orbitals involved in their bonding.

A reactivity factor to be analyzed and energy that is influenced influences the orbitals of a molecule on its own orbitals on nearby molecules, this energy is evaluated in the form of energy bands, which have direct dependence on chemical composition and molecular structure [26].

The band that comprises the highest and least busy levels of energy is called the conduction band, while the band consisting of the lowest energy occupied levels is called the valence band [27] [26] [28]. The region that exists between the valence band (orbital HOMO) and the conduction band (orbital LUMO) is called the gap, which corresponds to an energetically forbidden region to electrons. These energies can describe the electronic properties of a given molecule, such as its reactivity and the formation of charge transfer complexes. The formation of transition states is due to the interaction between the boundary orbitals of the reactive species [29].

Using the .out file generated by the structure optimization, the boundary orbitals, HOMO and LUMO were plotted, and the MESP was rendered.

To correlate structure and reactivity of molecules the values of the orbitals were used, the values of the orbital frontier were used to calculate the descriptors based on according to Koopman's Theory [30]: Gap, electron affinity (A), electronegativity (χ), vertical ionization potential (I), chemical hardness (η), chemical softness (s), electronic chemical potential (μ), electrophilicity index (ω) [31]. To obtain the values, the following formulas were used[32][33] [36][37][32]:

$$\text{GAP} \quad \Delta\varepsilon = |\varepsilon_{\text{HOMO}}| - |\varepsilon_{\text{LUMO}}| \quad (2)$$

$$\text{el ctron affinity (A)} \quad A = -\varepsilon_{\text{LUMO}} \quad (3)$$

$$\text{Vertical Ionization Potential (I)} \quad I = -\varepsilon_{\text{HOMO}} \quad (4)$$

$$\text{Eletronegativity } (\chi) \quad \chi = (I+A)/2 \quad (5)$$

$$\text{Chemical Hardness}(\eta) \quad \eta = (I-A)/2 \quad (6)$$

$$\text{Chemical Softness}(S) \quad S = 1/2\eta \quad (7)$$

$$\text{Eletronic Chemical Potential } (\mu) \quad \mu = - (I+A)/2 \quad (8)$$

$$\text{Electrophilicity Index } (\omega) \quad \omega = \mu^2 / 2\eta \quad (9)$$

In silico ADMET

The properties of Absorption, Distribution, Metabolization, Excretion and Toxicity (ADMET) including solubility, blood brain barrier (BHE), plasma protein binding, CYP2D6 binding, gastrointestinal absorption and hepatotoxicity were evaluated for in silico action of the Alternamide A compound by homology to other molecules that have already been studied in the human body. The models used to predict ADMET properties in this protocol are derived from various experimental data obtained for other drugs with similar chemical structure [38][39].

Prediction of drug similarity for Alternamide A for pharmacokinetics was performed on the Swiss ADME online platform of the Swiss Institute of Bioinformatics (<http://www.sib.swiss>). In the Swiss ADMET program package, the polar topological surface (TPSA) was calculated [40]. In addition, lipophilicity was predicted according to Wildman et al. [41], solubility and oral

bioavailability were assessed according to Lipinski and collaborators. [42] Analysis was performed to determine whether alternamide A was a cytochrome family isoform inhibitor (P450 CYP) such as CYP1A2 and CYP2D6. In addition to other pharmacokinetic prediction (gastrointestinal absorption, glycoprotein P and blood brain barrier) and prediction of similarity to drugs such as Ghose and Veber Rules and bioavailability [43]

3. Results and Discussions

As for the structure in question, Alternamide A, the MarvinSketch program was used to obtain the initial structure (figure 1) with an easily visible initial conformation, but with potential energy different from its native form and some other physical chemical properties (Table 1) necessary to study the structure in molecular modeling, highlighting the LogP partition coefficient (0.93), its density (1.371 ± 0.06 g / cm³), surface tension (58.9 ± 3.0 dyne / cm⁻¹), the solubility of the structure in water (0.06 mg / mL) that allowed defining the solvent (polar or non-polar) used in docking or molecular dynamics tests.

Table 1: Physicochemical Properties of Alkaloid Alternamide A

Property	Value	Property	Value
Solubility in water	0.06 mg/mL	Polar Surface Area	69.56 Å ²
LogP	0.93	Polarizability	22.36 Å ³
LogS	-1.4	Refractivity	58.29 m ³ ·mol ⁻¹
Molecular Formula	C ₁₂ H ₁₃ NO ₃	Density	1.371±0,06 g/cm ³
Superficial tension	58.9±3.0 dyne/cm	Molar Volume	159.8±3.0 cm ³
Monoisotopic Mass	219.089543 Da	Refractive index	1.639±0.02
Donors #H	3	#H Receivers	3

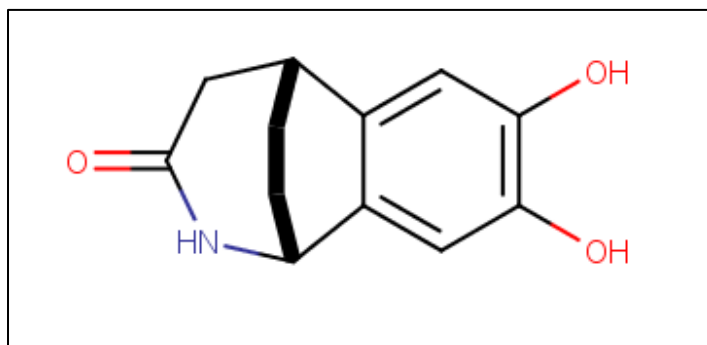


Figure 1: Alternamide A initial structure

Semiempirical methods have become a solution for modeling medium-sized molecules, as they use experimentally pre-established parameters, reducing the number of integrals to be solved for the Schrödinger equation solution (Equation 10)[44][45].

$$-\frac{\hbar^2}{2m} \nabla^2 \Psi + E_p \Psi = i\hbar \frac{\partial \Psi}{\partial t} \quad (10)$$

Since E_p is the potential energy in the region considered, m is the particle mass associated with this wave function and $\partial\psi / \partial t$ represents the partial derivative of the wave function in time order; $\nabla^2\Psi$ is the Laplacian mathematical operator of Ψ . Using the Born-Oppenheimer approximation, which decouples the electronic and nuclear movements, assuming a fixed position of the nuclei, the Schrödinger equation for the Alternamide A molecule was solved, having as a parameter the global energy state, where after a conformational analysis screening was obtained the configuration that can be considered more thermodynamically stable, which presented a self-consistent field energy (SCF) in the order of 3544,78775 eV (Figure 2), emphasizing that the self-consistent field theory, based on the assumption that the potential acting on each electron and due to the nuclei and the average charge distribution of the other electrons [46]. In order to characterize the behavior of the molecule against several solvents, the dipolar moment vector was calculated, using electronegativity values relative to each atom, calculates through the resulting vector, which globally calculates the magnitu of the charge displacement of each atom involved in the bond [47]. The alternamide molecule presented a dipole moment vector that showed values in the Cartesians of 0.84969627 (X axis), 2.31794357 (Y axis) and Z the value of -2.79671270 (Z axis), thus indicating a high polarity in the molecule, it is preferably soluble in polar solvents. With geometric optimization, the theoretically most stable molecule, it is also possible to calculate the formal and partial charges of each atom as well as its valence, despite the neutrality through optimization, it is possible to observe in the results obtained (table 2) the existence of charges partial (residual) charges that come from the electrons are closer or farther from one of the atoms of the bond, carrying charge. Note that carbon has a valence variation of 3 and 4, oxygen 1 and 2 and hydrogen has a valence of 1.

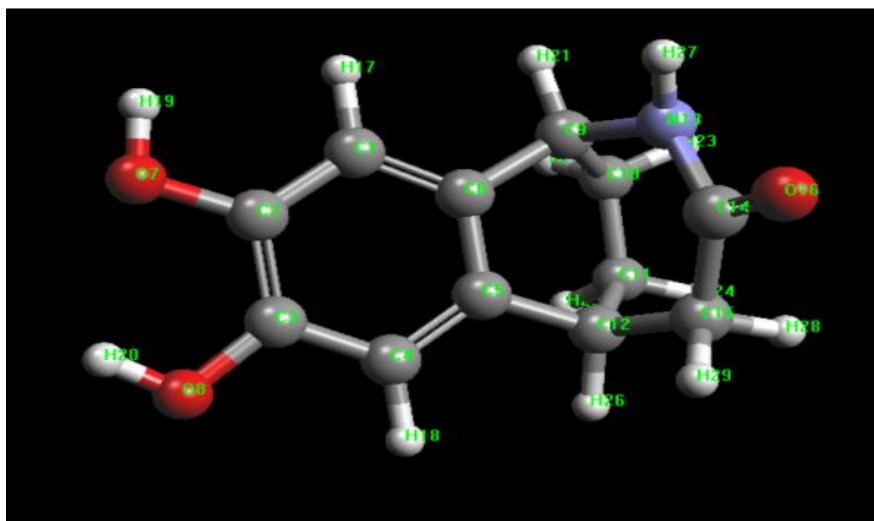


Figure 2: Optimized structure of Alternamide A tricyclic alkaloid

Table 2: Atomic properties of alternamide A

Atom	Elemento/type		Valence	Partial charge
1	C	Car	3	-0.011
2	C	Car	3	0.159
3	C	Car	3	0.159
4	C	Car	3	-0.013
5	C	Car	3	-0.035

6	C	Car	3	-0.020
7	O	O3	2	-0.503
8	O	O3	2	-0.503
9	C	C3	4	0.049
10	C	C3	4	-0.030
11	C	C3	4	-0.044
12	C	C3	4	-0.007
13	N	Nam	3	-0.308
14	C	C2	3	0.214
15	C	C3	4	0.031
16	O	O2	1	-0.276
17	H	H	1	0.066
18	H	H	1	0.066
19	H	Ho	1	0.292
20	H	Ho	1	0.292
21	H	H	1	0.055
22	H	H	1	0.029
23	H	H	1	0.029
24	H	H	1	0.027
25	H	H	1	0.027
26	H	H	1	0.035
27	H	H	1	0.149
28	H	H	1	0.036
29	H	H	1	0.036

Analyzing the bonds, it was possible to observe a predominance of the predominantly covalent bonds, where we can highlight the bonds between carbon (C4 - C3), (C5 - C6), (C2 - C1) and oxygen-carbon (C11 - O3) as second order bonds, and the bonds between carbon (C8 - C9), (C9 - C10), (C8 - C7), (C10 - C12) because they are rotatable, as we can see in table 4.

Table 4: Alternamide A binding properties

Bond	Type	Start storm	End storm	Bond order	Rotable	Length(Å)
1	H-C	H9	C9	1	No	1.10751
2	H-C	H6	C8	1	No	1.10738
3	C-H	C9	H8	1	No	1.10772
4	C-C	C9	C8	1	Yes	1.52898
5	C-C	C9	C10	1	Yes	1.5348
6	H-C	H10	C10	1	No	1.11838
7	C-H	C8	H7	1	No	1.10775
8	C-C	C8	C7	1	Yes	1.53845
9	H-C	H2	C4	1	No	1.09719
10	O-H	O2	H4	1	No	0.95015
11	O-C	O2	C3	1	No	1.36922
12	C-C	C4	C3	2	No	1.40217
13	C-C	C4	C5	1	No	1.39074

14	C-C	C3	C2	1	No	1.41347
15	C-C	C10	C5	1	No	1.50161
16	C-C	C10	C12	1	Yes	1.53300
17	C-C	C5	C6	2	No	1.39989
18	C-O	C2	O1	1	No	1.37677
19	C-C	C2	C1	2	No	1.93354
20	O-H	O1	H3	1	No	0.95045
21	C-C	C6	C1	1	No	1.39035
22	C-C	C6	C7	1	No	1.5052
23	C-H	C1	H1	1	No	1.09738
24	C-H	C7	H5	1	No	1.11803
25	C-N	C7	N	1	No	1.49525
26	H-C	H12	C12	1	No	1.10973
27	C-H	C12	H13	1	No	1.10936
28	C-C	C12	C11	1	No	1.51678
29	N-C	N	C11	1	No	1.42795
30	N-H	N	H11	1	No	1.00008
31	C-O	C11	O3	2	No	1.22503

Regarding the angles, we can highlight the connection angles that were in the range of 105.4833° (H- C8 - H7) and 124.5218° (C2 - C3 - O2) (table 5). The torsion angles were between -0.0181° (H2 - C4 - C5 - C6) and -179.9801° (C3 - C2 - C1 - H1) (Table 6).

Table 5: Alternamide A lead angles

Angle	Type	Start Atom	Vertex	End Atom	Angle ($^\circ$)
1	CCC	C2	C1	C6	119.1211
2	CCH	C2	C1	H1	120.7349
3	CCH	C6	C1	H1	120.1439
4	CCO	C3	C2	O1	117.0555
5	CCC	C1	C2	C3	120.3501
6	CCO	C1	C2	O1	122.5941
7	CCO	C4	C3	O2	115.5915
8	CCO	C2	C3	O2	124.5218
9	CCC	C2	C3	C4	119.8851
10	CCH	C3	C4	H2	120.1964
11	CCH	C5	C4	H2	120.5386
12	CCC	C3	C4	C5	119.2650
13	CCC	C4	C5	C10	122.3942
14	CCC	C4	C5	C6	120.6718
15	CCC	C6	C5	C10	116.9283
16	CCC	C1	C6	C5	120.7060
17	CCC	C5	C6	C7	116.7266
18	CCC	C1	C6	C7	122.5674
19	COH	C2	O1	H3	107.3513
20	COH	C3	O2	H4	108.7348

21	CCC	C6	C7	C8	110.0866
22	CCH	C8	C7	H5	108.6699
23	CCN	C8	C7	N	110.3696
24	CCH	C6	C7	H5	110.2542
25	CCN	C6	C7	N	111.3233
26	NCH	N	C7	H5	106.0327
27	CCH	C9	C8	H6	109.4691
28	HCH	H6	C8	H7	105.4833
29	CCH	C7	C8	H6	108.1887
30	CCH	C9	C8	H7	110.2405
31	CCC	C7	C8	C9	113.4651
32	CCH	C7	C8	H7	109.6657
33	HCH	H8	C9	H9	105.4865
34	CCH	C8	C9	H9	109.3703
35	CCH	C10	C9	H9	108.5279
36	CCH	C8	C9	H8	110.1961
37	CCH	C10	C9	H8	109.3253
38	CCC	C8	C9	C10	113.6036
39	CCH	C9	C10	H10	107.8414
40	CCC	C5	C10	C9	109.4995
41	CCC	C9	C10	C12	111.9786
42	CCH	C5	C10	H10	109.2003
43	CCH	C12	C10	H10	106.9915
44	CCC	C5	C10	C12	111.2100
45	CNC	C7	N	C11	121.1514
46	CNH	C7	N	H11	111.9097
47	CNH	C11	N	H11	113.9215
48	NCC	N	C11	C12	122.9328
49	CCO	C12	C11	O3	121.9509
50	NCO	N	C11	O3	114.9630
51	CCH	C10	C12	H12	109.3249
52	CCH	C10	C12	H13	108.7719
53	CCC	C10	C12	C11	117.1743
54	HCH	H12	C12	H13	105.7666
55	CCH	C11	C12	H12	107.5057
56	CCH	C11	C12	H13	107.7090

Table 6: Torsion angles of alternamide A

Torsion	Type	Atom 1	Atom 2	Atom 3	Atom 4	Torsion (°)
1	HCCH	H9	C9	C8	H6	-2.3992
2	HCCH	H9	C9	C8	H7	-118.0022
3	HCCC	H9	C9	C8	C7	118.5569
4	HCCH	H8	C9	C8	H6	113.1256
5	HCCH	H8	C9	C8	H7	-2.4774

6	HCCC	H8	C9	C8	C7	-125.9183
7	CCCH	C10	C9	C8	H6	-123.8126
8	CCCH	C10	C9	C8	H7	120.5843
9	CCCC	C10	C9	C8	C7	-2.8566
10	HCCH	H9	C9	C10	H10	45.8811
11	HCCC	H9	C9	C10	C5	-72.8358
12	HCCC	H9	C9	C10	C12	163.3298
13	HCCH	H8	C9	C10	H10	-68.6982
14	HCCC	H8	C9	C10	C5	172.5849
15	HCCC	H8	C9	C10	C12	48.7505
16	CCCH	C8	C9	C10	H10	167.7639
17	CCCC	C8	C9	C10	C5	49.0470
18	CCCC	C8	C9	C10	C12	-74.7875
19	HCCC	H6	C8	C7	C6	76.4556
20	HCCH	H6	C8	C7	H5	-44.3845
21	HCCN	H6	C8	C7	N	-160.2609
22	CCCC	C9	C8	C7	C6	-45.2182
23	CCCH	C9	C8	C7	H5	-166.0583
24	CCCN	C9	C8	C7	N	78.0654
25	HCCC	H7	C8	C7	C6	-168.9732
26	HCCH	H7	C8	C7	H5	70.1867
27	HCCN	H7	C8	C7	N	-45.6897
28	HOCC	H4	O2	C3	C4	177.5188
29	HOCC	H4	O2	C3	C2	-2.9488
30	HCCO	H2	C4	C3	O2	-0.2085
31	HCCC	H2	C4	C3	C2	-179.7641
32	CCCO	C5	C4	C3	O2	179.7198
33	CCCC	C5	C4	C3	C2	0.1641
34	HCCC	H2	C4	C5	C10	0.9175
35	HCCC	H2	C4	C5	C6	-179.9801
36	CCCC	C3	C4	C5	C10	-179.0105
37	CCCC	C3	C4	C5	C6	0.0920
38	OCCO	O2	C4	C2	O1	0.1050
39	OCCC	O2	C4	C2	C1	-179.7159
40	CCCO	C4	C3	C2	O1	179.6185
41	CCCC	C4	C3	C2	C1	-0.2023
42	CCCC	C9	C10	C5	C4	130.6111
43	CCCC	C9	C10	C5	C6	-48.5230
44	HCCC	H10	C10	C5	C4	12.7399
45	HCCC	H10	C10	C5	C6	-166.3942
46	CCCC	C12	C10	C5	C4	-105.1044
47	CCCC	C12	C10	C5	C6	75.7615
48	CCCH	C9	C10	C12	H12	-47.4345
49	CCCH	C9	C10	C12	H13	-162.4782

50	CCCC	C9	C10	C12	C11	75.1360
51	HCCH	H10	C10	C12	H12	70.5220
52	HCCH	H10	C10	C12	H13	-44.5217
53	HCCC	H10	C10	C12	C11	-166.9075
54	CCCH	C5	C10	C12	H12	-170.3048
55	CCCH	C5	C10	C12	H13	74.6515
56	CCCC	C5	C10	C12	C11	-47.7342
57	CCCC	C4	C5	C6	C1	-0.3172
58	CCCC	C4	C5	C6	C7	179.6343
59	CCCC	C10	C5	C6	C1	178.8328
60	CCCC	C10	C5	C6	C7	-1.2157
61	CCOH	C3	C2	O1	H3	178.1454
62	CCOH	C1	C2	O1	H3	-2.0381
63	CCCC	C3	C2	C1	C6	-0.0181
64	CCCH	C3	C2	C1	H1	179.8879
65	OCCC	O1	C2	C1	C6	-179.8288
66	OCCH	O1	C2	C1	H1	0.0772
67	CCCC	C5	C6	C1	C2	0.2762
68	CCCH	C5	C6	C1	H1	-179.6304
69	CCCC	C7	C6	C1	C2	-179.6724
70	CCCH	C7	C6	C1	H1	0.4210
71	CCCC	C5	C6	C7	C8	49.1511
72	CCCH	C5	C6	C7	H5	169.0354
73	CCCN	C5	C6	C7	N	-73.5733
74	CCCC	C1	C6	C7	C8	-130.8984
75	CCCH	C1	C6	C7	H5	-11.0141
76	CCCN	C1	C6	C7	N	10.3772
77	CCNC	C8	C7	N	C11	-76.2674
78	CCNH	C8	C7	N	H11	144.8117
79	CCNC	C6	C7	N	C11	46.2942
80	CCNH	C6	C7	N	H11	-92.6267
81	HCNH	H5	C7	N	C11	166.2174
82	HCNH	H5	C7	N	H11	27.2965
83	CCCN	C10	C12	C11	N	-26.4625
84	CCCO	C10	C12	C11	O3	158.2655
85	HCCN	H12	C12	C11	N	97.0395
86	HCCO	H12	C12	C11	O3	-78.2325
87	HCCN	H13	C12	C11	N	-149.3947
88	HCCO	H13	C12	C11	O3	35.3333
89	CNCC	C7	N	C11	C12	27.3855
90	CNCO	C7	N	C11	O3	-157.0390
91	HNCC	H11	N	C11	C12	165.551
95	HNCO	H11	N	C11	O3	-18.8694

For load analysis of the molecules, the Mulliken population analysis [48], which has its algorithms based on the theory of molecular orbitals, using a linear combination of atomic orbitals (with coefficients determined by the Hartree-Fock method) [49], was used to define a set of molecular orbitals, it is possible to obtain a partition scheme, which distributes the electrons in the atoms, being used to predict and characterize the possible intra and intermolecular interactions of the molecule, being an important descriptor for the correlational study of the structure and the molecular structure. its biological activity [50] [51]. By analyzing the population distribution of charges, Alternamide A showed a variation between atomic charges of atoms of the same element, as the carbon with the highest charge was C14 with a value of 0.2781 while the lowest charge was the C15 with a value of 0.2781 from -0.2640, ranging from 0.5421 load; the same way oxygen with the highest load was O8 with -0.2349 and the lowest oxygen was O16 with -0.3892, varying 0.1543; As for hydrogen, atomic charges ranged from 0.1249 in H25 to 0.2384 in H20 hydrogen, showing a variation of 0.1135, inferring that these variations are directly related to the electronegativity differences of atoms (table 7).

Table 7: Mulliken population analysis, showing Mulliken atomic charges for alternamide A atoms C, O and H.

Atom	Charge	Atom	Charge
01 C	-0.2140	16 O	-0.3892
02 C	-0.0037	17 H	0.1984
03 C	0.0706	18 H	0.2209
04 C	-0.1986	19 H	0.2357
05 C	-0.0706	20 H	0.2384
06 C	-0.1294	21 H	0.1370
07 O	-0.2548	22 H	0.1253
08 O	-0.2349	23 H	0.1379
09 C	-0.0514	24 H	0.1253
10 C	-0.2391	25 H	0.1249
11 C	-0.2314	26 H	0.1450
12 C	-0.0883	27 H	0.1400
13 N	-0.1207	28 H	0.1522
14 C	0.2781	29 H	0.1574
15 C	-0.2640		

Using the data generated in structural optimization, molecular modeling techniques also contribute to the understanding of intermolecular interactions through the study of electrostatic potential surface maps (MESP) [26] [52]. three-dimensional charge distribution, being important for the analysis and identification of regions with higher and lower electron density, being a strong indicator of nucleophilic and electrophilic sites, being important to analyze descriptors of molecular interactions with polarity and electronegativity, that is, a descriptor capable of assisting in the behavior of molecules against other charged molecules [25][53]. The region with the highest electrostatic potential is indicative of a low negative charge density, which can be understood as a low electron density. Usually, but not always, the color red indicates the lowest potential electrostatic energy, which characterizes a region with higher electron density. The white region represents the largest electrostatic energy, indicating a relative absence of electrons. Intermediate

colors, green and yellow, represent an intermediate electrostatic potential [54]. Using the three-dimensional coordinates of the optimized structure and the charges was rendered the Alternamide A electrostatic potential map, showed a well-wasted distribution of electrostatic potential, where it was possible to identify a higher electron density (nucleophilic region) represented in red, located in the vicinity of oxygen atoms (figure 3), which is indicative of a region in quantity of electrons, being astas the possible places of interaction through electrostatic interactions due to hydrogen bonds.

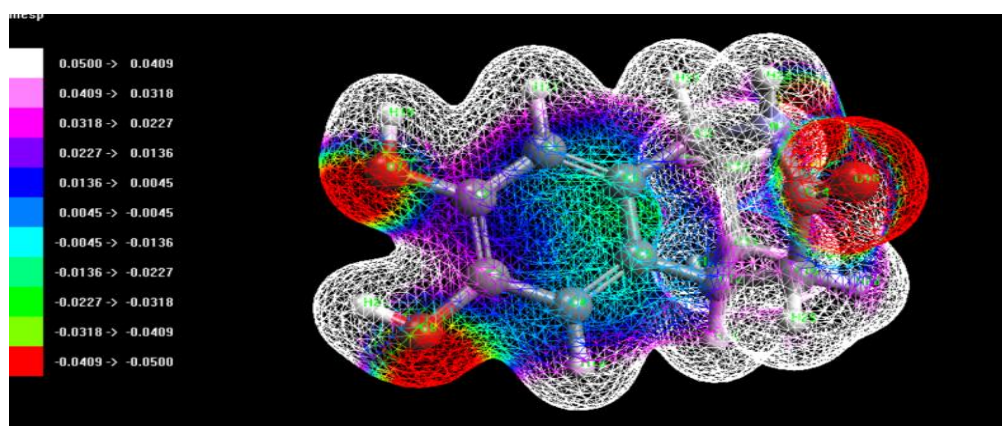


Figure 3: Electrostatic Potential Map rendered from the semi-empirical quantum method using the PM3 parameterization.

Boundary orbitals have been widely related as descriptors of molecule reactivity, because in their theory the transition state formation is due to the interaction between the HOMO (highest occupied molecular orbital) and LUMO (lowest unoccupied molecular orbital) of the species. These are the descriptors that broadly characterize the nature of chemical reactions, since the energy of HOMO is directly related to the susceptibility of the molecule to undergo an electrophilic attack (ionization potential), and the energy of LUMO to susceptibility nucleophile attacks (electron affinity) [55] [56] [57]. In the alternamide molecule it was possible to observe the presence of 77 molecular orbitals and it is possible to identify Homo as number 42, which was symmetrical between its negative (red) and positive (blue) phases, with a strong contribution of oxygen atoms and ligados-bonded atoms el, having an energy of -0.333062 ev. The homo orbital, also symmetrical between the phases, was identified as the orbital 43, with energy in the order of -0.002131 eV, which is formed by the major contribution of the ligados-bonded atoms present in the ring (figure 4).

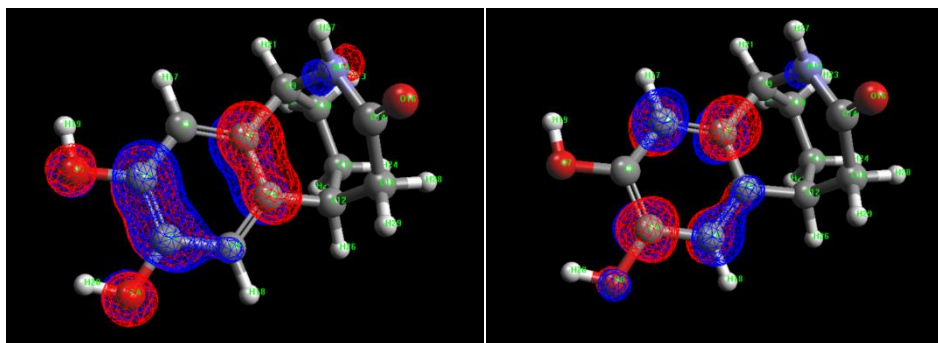


Figure 4: Boundary molecular orbitals, rendered using the semi-empirical quantum method, with parameterization PM3. Fig. 4A (HOMO orbital) and Fig. 4B (LUMO orbital) respectively.

The GAP energy difference (ΔE) between HOMO and LUMO orbitals may be related to chemical stability, as a large difference would be indicative of high stability (low reactivity), while a low gap value indicates a high reactivity, as it indicates a low energy value for chemical transition, that is, it indicates the electron-donor and / or electron-acceptor character of a compound [58]. Alternamide had a gap in the order of 0.330931, with ionization potential in the order of To characterize better it was possible to calculate an ionization potential (I) in the order of 0.333062 eV, ie the minimum energy required to remove an electron of alternamide A with respect to energy change when an electron is added to a neutral atom in the gas phase. Electron affinity (A) is described as the change in energy when an electron is added to a neutral atom in the gas phase was predicted to be a small value on the order of 0.002131 eV. Noting that low I values may be indicative of a charge transfer mechanism between a ligand-receptor interaction. Another important descriptor to characterize this interaction and electronegativity (χ), which for alternamide was of the order of 0.167597 eV, which is the estimated ability of a molecule to attract electrons from another molecule in a chemical interaction [59].

Using the values of HOMO and Lumo it was possible to calculate the descriptors of polarizability chemical softness (S) 3.021777954, chemical hardness (η) 0.1665466 ev, thus characterizing althernamide A as a high reactivity molecule, requiring a small amount of energy for a transition of an electron from HOMO to LUMO [60].

Regarding the bioavailability (Figure 5) of the molecule shown in the color zone is the appropriate physicochemical space for oral bioavailability, where the following properties were taken into account as flexibility, lipophilicity, saturation, size, polarity and solubility. The lipophilicity of the studied compound log P may range from -0.7 to +5.0. Molecular weight may range from 150 g / mol to 500 g / mol. The topological polar surface area ranges from 20-130 A². Insolubility was studied using log S (ESOL) and ranged from 0 to 6. The number of rotational bonds should be between 0-9 and the unsaturation fraction ranges from 0.25 to 1.0, indicating the fraction of carbon atoms. sp³ hybridization should not be less than 0.25 [61] [62].

The physicochemical properties show that the molecule C₁₂H₁₃NO₃. The molecular weight was 219.24 g / mol. The number of heavy atoms is 16 and 6 the number of aromatics. The fraction of carbon atoms in sp³ hybridization was 0.42. Meanwhile, the number of hydrogen bond acceptors was 3 and the number of hydrogen bond donor was 3. The molar refractivity was 62.34 and the topological polar surface area found was 69.56 A².

The log Po/w (ilog P) is 1.32, the log Po/w (Xlog P₃) is 0.61, the log Po/w (Wlog P) is 0.83, the log Po/w (MlogP) is 0.86 the logPo/w (SILICOS-IT) is 1.32 and the consensus log Po/w is 1.00 respectively. From the log P values overall it can be concluded that the compound is having good lipophilic character. The water solubility of the compound was studied using log S (ESOL) value as -1.83 depicting the compound belongs to very soluble water class [63].

The pharmacokinetic properties were studied using the BOILED-Egg model [64] to simulate an intuitive assessment of passive gastrointestinal absorption (HIA) and brain barrier permeation (BBB) as a function of the position of molecules in the WLOGP-versus-TPSA framework (Figure 6). If the substance is in the white region, it indicates that it has a high probability of passive

absorption by the gastrointestinal tract, whereas if it is in the yellow region, it indicates that it has a high probability of brain permeation [65] [40].

The Alternamide A molecule showed high gastrointestinal absorption, however it does not easily permeate the brain barrier. It is a P-gp substrate meaning there may be problem excreting the drug. For, P-glycoprotein plays a significant role in drug absorption and distortion. Due to its location, P-glycoprotein appears to have a greater impact on limiting drug uptake of blood circulation in the brain and intestinal lumen in epithelial cells than in increasing drug excretion of hepatocytes and renal tubules in the adjacent luminal space. The substance is not an inhibitor of CYP2C19 and CYP2D6 isoenzyme, which means that there is no chance of drug accumulation or interaction resulting in toxicity. The similarity parameter of the drug is high because it follows the rule of Lipinski, Verber, Egan, with a bioavailability score of 0.55. The SWISS ADME Synthetic Accessibility (SA) score is based primarily on the supposed frequency of molecular fragments in obtained molecules correlates with ease of synthesis. The fragmentary contribution to (SA) should be favorable for frequent and unfavorable chemical portions for rare portions. The synthetic accessibility score was 2.75, which means that the molecule has great viability to be synthesized.

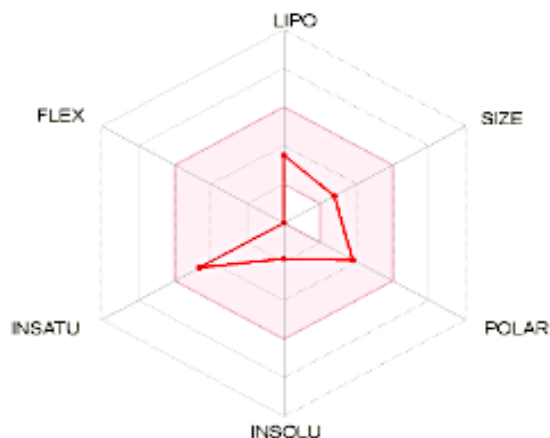


Figure 5: The bioavailability of Alternamide A using Swiss ADME predictor

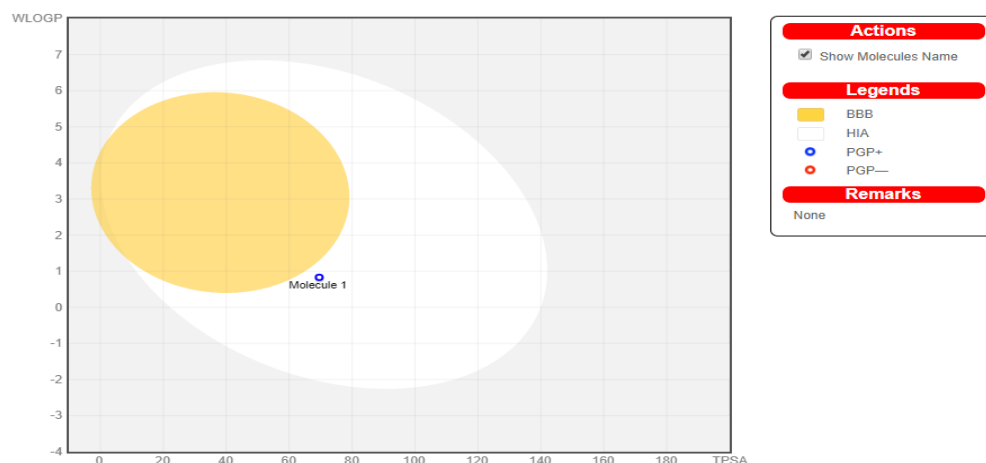


Figure 6: Molecule falling in BOILED-Egg is predicting the molecule is able to penetrate through the blood brain barrier.

4. Conclusions

Using the semi-empirical quantum formalism it was possible to identify the most stable conformation of the tricyclic alkaloid alternamide A, the boundary orbitals, calculate to identify the nucleophilic sites and the reactivity descriptors. Through *in silico* absorption, distribution, metabolism, excretion and toxicity (ADMET) simulations, including solubility, blood-brain barrier (BBB), plasma protein binding, CYP2D6 binding, gastrointestinal absorption and hepatotoxicity, it was observed that good oral bioavailability and high water solubility high gastrointestinal absorption. The synthetic accessibility score was 2.75, which means that it would be easy to synthesize the molecule under study. Highlighting what the present study represents as a fundamental step for future molecular docking and drug design studies for the development of *T-cruzi* evolutionary form inhibitors.

Acknowledgements

The present work was partially funded by CNPq - National Council for Scientific and Technological Development and CAPES - Brazilian Federal Agency for Support and Evaluation of Postgraduate Education of the Brazilian Ministry of Education.

References

- [1] Dias, L.C., Dessoy, M.A., Silva J.J.N., Thiemann O.H., Oliva G., Andricopulo A.D. Chemotherapy of Chagas' disease: State of the art and perspectives for the development of new drugs. Quim Nova. 2009;
- [2] Bermudez, J., Davies, C., Simonazzi, A., Pablo Real, J., Palma, S., Current drug therapy and pharmaceutical challenges for Chagas disease. Acta Tropica. 2016.
- [3] Coura, J.R. Ripanosomose, doença de. E N D E M I a S / a R T I G O S. 1999;
- [4] De Oliveira Filho, G.B., Cardoso, M.V., Espíndola, J.W.P., Oliveira e Silva, D.A., Ferreira, R.S., Coelho, P.L., et al. Structural design, synthesis and pharmacological evaluation of thiazoles against *Trypanosoma cruzi*. Eur J Med Chem. 2017;
- [5] Repetto, E.C., Zachariah, R., Kumar, A., Angheben, A., Gobbi, F., Anselmi, M., et al. Neglect of a Neglected Disease in Italy: The Challenge of Access-to-Care for Chagas Disease in Bergamo Area. PLoS Negl Trop Dis. 2015;
- [6] Moncayo, A., Silveira, A.C. Current epidemiological trends of Chagas disease in Latin America and future challenges: Epidemiology, surveillance, and health policies. In: American Trypanosomiasis Chagas Disease: One Hundred Years of Research: Second Edition. 2017.
- [7] De Menezes, R.P.B., Sampaio, T.L., Lima, D.B., Sousa, P.L., De Azevedo, I.E.P., Magalhães, E.P., et al. Antiparasitic effect of (-)- α -bisabolol against *Trypanosoma cruzi* Y strain forms. Diagn Microbiol Infect Dis [Internet]. 2019:114860. Available from: <https://doi.org/10.1016/j.diagmicrobio.2019.06.012>
- [8] Koolen, H.H.F., Pral, E.M.F., Alfieri, S.C., Marinho, J.V.N., Serain, A.F., Hernández-Tasco, A.J., Antiprotozoal and antioxidant alkaloids from *Alternanthera littoralis*. Phytochemistry. 2017;
- [9] Lima, A.R., Silva, J., Bezerra, L.L., Marinho, M.M., Marinho, E.S. Molecular docking of potential curcuminoids inhibitors of the NS1 protein of dengue virus. Int J Sci Eng Res. 2017;8(4).
- [10] Carneiro, S.S., Lima, A.R., Marinho, M.M., Marinho, E.S. In silico Study Of The Therapeutic Agent In The Treatment Of Non-Hodgkin' s Lymphomas, Peripheral T- Cell Belinostat , A Semi-Empirical Approach. Imp J Interdiscip Res. 2016;(8):1645–8.

- [11] Oliveira, V.M. De, Marinho, M.M., Marinho, E.S., Semi-Empirical Quantum Characterization of the Drug Selexipag: HOMO and LUMO and Reactivity Descriptors. *Int J Recent Res Rev.* 2019; XII (2):15–20.
- [12] Henrique, C., Roberto, A., Marinho, E.S., Campos, O.S., Nithael, F., Lucio M, Characterization of the natural insecticide methylcytisine: An in silico study using classic force field. *Int J Recent Res Rev.* 2019; XII (2):15–20.
- [13] Cheng, F., Li, W., Zhou, Y., Shen, J., Wu, Z., Liu, G., et al. AdmetSAR: A comprehensive source and free tool for assessment of chemical ADMET properties. *J Chem Inf Model.* 2012;
- [14] Tareq-Hassan Khan, M. Predictions of the ADMET Properties of Candidate Drug Molecules Utilizing Different QSAR/QSPR Modelling Approaches. *Curr Drug Metab.* 2010;
- [15] Chinthala, Y., Thakur, S., Tirunagari, S., Chinde, S., Domatti, A.K., Arigari, N.K., et al. Synthesis, docking and ADMET studies of novel chalcone triazoles for anti-cancer and anti-diabetic activity. *Eur J Med Chem.* 2015;
- [16] Atkins, P., De Paula, J. *Atkins' physical chemistry / Peter Atkins, Julio de Paula. Physical chemistry.* 2010.
- [17] Lopes, D., Oliveira, S. De, Marinho, M.M., Marinho, E. S., Butanamide. Characterization in Silico of Anti-Epileptic Drug (2S)-2-[(4R)-2-(propylpyrrolidin-1-yl)]-. 2018; XI(4):5–12.
- [18] Csizmadia, P. MarvinSketch and MarvinView: Molecule Applets for the World Wide Web. In 2019.
- [19] Thompson, M.A., ArgusLab 401. Planaria Software LLC, Seattle, WA. ArgusLab 4.0. 1. Seattle; 2010.
- [20] Thompson, J.D., Cramer, C.J., Truhlar, D.G. Parameterization of charge model 3 for AM1, PM3, BLYP, and B3LYP. *J Comput Chem.* 2003;
- [21] Hanwell, M.D., Curtis, D.E., Lonie, D.C., Vandermeersch, T., Zurek, E., Hutchison, G.R. Avogadro: An advanced semantic chemical editor, visualization, and analysis platform. *J Cheminform.* 2012;
- [22] Reges, M., Marinho, M.M., Marinho, E.S. Semi-Empirical Study of the Drug Riociguat, an Important Drug for Oral Treatment against Chronic Thromboembolic Pulmonary Hypertension. *Int J Sci Eng Sci.* 2017;1(1):13–7.
- [23] Araujo, G.A., Silva, E.P., Sanabio, R.G., Pinheiro, J.A., Albuquerque, M.B., Castro, R.R., et al. Characterization in Silico of the Structural Parameters of the Antifungal Agent Ketoconazole. *Biol Chem Res.* 2016;
- [24] Paes, L., Santos, W.L., Marinho, M.M., Marinho, E.S. ESTUDO DFT DO ALCALOIDE DICENTRINA: GAP, HOMO, LUMO, MESP E MULLIKEN. *JOIN.* 2017;(1).
- [25] Prabavathi, N., Nilufer, A., Krishnakumar, V. Molecular structure, vibrational, UV, NMR, hyperpolarizability, NBO and HOMO-LUMO analysis of Pteridine2,4-dione. *Spectrochim Acta - Part A Mol Biomol Spectrosc.* 2012;
- [26] Mulliken, R.S. Electronic population analysis on LCAO-MO molecular wave functions. I. *J Chem Phys.* 1955;
- [27] Atkins, P.W., Overton, T., Rourke, J., Weller, M., Armstrong, F., Hagerman, M. Shriver & Atkins' *Inorganic Chemistry.* Shriver and Atkin's inorganic chemistry. 2010.
- [28] Gopakumar, T.G., Meiss, J., Pouladsaz, D., Hietschold, M. HOMO-LUMO gap shrinking reveals tip-induced polarization of molecules in ultrathin layers: Tip-sample distance-dependent scanning tunneling spectroscopy on d8 (Ni, Pd, and Pt) phthalocyanines. *J Phys Chem C.* 2008;
- [29] Suresh, Kumar. S., Athimoolam, S., Sridhar, B. XRD, vibrational spectra and quantum chemical studies of an anticancer drug: 6-Mercaptopurine. *Spectrochim Acta - Part A Mol Biomol Spectrosc.* 2015;
- [30] Koopmans, T. Über die Zuordnung von Wellenfunktionen und Eigenwerten zu den Einzelnen Elektronen Eines Atoms. *Physica.* 1934;

- [31] Vijayaraj, R., Subramanian, V., Chattaraj, P.K. Comparison of global reactivity descriptors calculated using various density functionals: A QSAR perspective. *J Chem Theory Comput.* 2009;
- [32] Chermette, H. Chemical reactivity indexes in density functional theory. *J Comput Chem.* 1999;
- [33] Padmanabhan, J., Parthasarathi, R., Subramanian, V., Chattaraj, P.K. Electrophilicity-based charge transfer descriptor. *J Phys Chem A.* 2007;
- [34] Chattaraj, P.K., Sarkar, U. *Theoretical Aspects of Chemical Reactivity. Theoretical and Computational Chemistry.* 2007.
- [35] Parr, R.G., Pearson R.G. Absolute hardness: companion parameter to absolute electronegativity. *J Am Chem Soc* [Internet]. 1983 Dec;105(26):7512–6. Available from: <http://pubs.acs.org/doi/abs/10.1021/ja00364a005>
- [36] Parr, R.G., Chattaraj, P.K. Principle of Maximum Hardness. *J Am Chem Soc.* 1991;
- [37] Lee, C., Yang, W., Parr, R.G. Into a Functional of the Electron Density F . *Phys Rev B.* 1988;
- [38] Okoli, P.T, Nzute, V.C, Durojaye, O.A., Chiello, O.H., Ajibo, Q.C., Udo, S.I., et al. An In-silico Pharmacokinetics Study on Cis- A Nutraceutical Compound with Anticancer Properties. 2019;7(3):1–7.
- [39] Silva, A.B.F, Marinho M.M., Mendes F.R.D.S. In Silico Study of Phytochemical Chlorogenic Acid: A Semi- Empirical Quantum Study and Adme. *Int J Recent Res Rev.* 2019; XII (2):34–9.
- [40] Daina, A., Michielin, O., Zoete, V. SwissADME: A free web tool to evaluate pharmacokinetics, drug-likeness and medicinal chemistry friendliness of small molecules. *Sci Rep.* 2017;
- [41] Wildman, S.A, Crippen, G.M. Prediction of physicochemical parameters by atomic contributions. *J Chem Inf Comput Sci.* 1999;
- [42] Lipinski, C.A, Lombardo, .F, Dominy, B.W., Feeney, P.J. Experimental and computational approaches to estimate solubility and permeability in drug discovery and development settings. *Advanced Drug Delivery Reviews.* 2012.
- [43] Waring, M.J. Defining optimum lipophilicity and molecular weight ranges for drug candidates- Molecular weight dependent lower log D limits based on permeability. *Bioorganic Med Chem Lett.* 2009;
- [44] Lewars, E.G. *Computational chemistry: Introduction to the theory and applications of molecular and quantum mechanics: Third Edition 2016. Computational Chemistry: Introduction to the Theory and Applications of Molecular and Quantum Mechanics: Third Edition 2016.* 2016.
- [45] Marinho, E.S. Utilização Do Método Semi-Empírico Pm7 Para Caracterização Do Fármaco Atalurenol : Homo ,. *Rev Expressão Católica.* 2016;1(1):177–84.
- [46] Atkins, P., Paula, J. de, Friedman, R.. *Quanta, Matter, and Change: A molecular approach to physical chemistry.* New York. 2009;
- [47] Atkins, P., Friedman, R., *Molecular Quantum Mechanics Fourth Edition.* Oxford Univ Press New York. 2005;
- [48] Eryilmaz, S., Gül, M., Inkaya, E., Taş, M. Isoxazole derivatives of alpha-pinene isomers: Synthesis, crystal structure, spectroscopic characterization (FT-IR/NMR/GC-MS) and DFT studies. *J Mol Struct.* 2016;
- [49] Morgon, N.H., Custodio, R., Custódio, R., Morgan, N. H. and Custódio, R. Teoria do Funcional da Densidade. *Quim Nov* [Internet]. 1995;18(1):44. Available from: http://quimicanova.s bq.org.br/qn/qnol/1995/vol18n1/v18_n1_10.pdf
- [50] Reges, M., Marinho, M.M., Marinho, E.S. Structural Characterization of the Hypoglycemic Drug Glimperiride. *Int J Recent Res Rev.* 2018; XI (2):26–35.
- [51] Carneiro, S.S., Marinho, M.M., Marinho, E.S. Electronic / Structural Characterization of Antiparkinsonian Drug Istradefylline : A Semi-Empirical Study. *Int J Recent Res Rev.* 2017; X (4):9–14.
- [52] Marinho ES. A DFT study of synthetic drug topiroxostat: MEP, HOMO, LUMO. *Int J Sci Eng Res.* 2016;7(July):1264–70.

- [53] Eyre, R.J., Goss, J.P, MacLeod, R.M., Briddon, P.R. Stability of singly hydrated silanone on silicon quantum dot surfaces: Density functional simulations. *Phys Chem Chem Phys*. 2008;
- [54] Mohan, N., Suresh, C.H. A molecular electrostatic potential analysis of hydrogen, halogen, and dihydrogen bonds. *J Phys Chem A*. 2014;
- [55] Lai, T.Y, Guo, J.D., Fettinger, J.C., Nagase, S., Power, P.P. Facile insertion of ethylene into a group 14 element-carbon bond: effects of the HOMO-LUMO energy gap on reactivity. *Chem Commun*. 2019;
- [56] Rottschäfer, D., Sharma, M.K., Neumann, B., Stammler, H.G., Andrada, D.M., Ghadwal, R.S. A Modular Access to Divinyldiphosphenes with a Strikingly Small HOMO–LUMO Energy Gap. *Chem - A Eur J*. 2019;
- [57] AlAbbad, S., Sardot, T., Lekashvili, O., Decato, D., Lelj F., Ross J.B.A., et al. Trans influence and substituent effects on the HOMO-LUMO energy gap and Stokes shift in Ru mono-diimine derivatives. *J Mol Struct*. 2019;
- [58] The Theoretical Prediction of Thermophysical properties, HOMO, LUMO, QSAR and Biological Indics of Cannabinoids (CBD) and Tetrahydrocannabinol (THC) by Computational Chemistry. *Adv J Chem A*. 2019;
- [59] Arroio, A., Honório, K.M., Da Silva, A.B.F. Propriedades químico-quânticas empregadas em estudos das relações estrutura-atividade. *Quimica Nova*. 2010.
- [60] Rajan, V.K., Muraleedharan, K. A computational investigation on the structure, global parameters and antioxidant capacity of a polyphenol, Gallic acid. *Food Chem [Internet]*. 2017;220:93–9. Available from: <http://dx.doi.org/10.1016/j.foodchem.2016.09.178>
- [61] Ferreira, L.L.G, Andricopulo, A.D. ADMET modeling approaches in drug discovery. *Drug Discovery Today*. 2019.
- [62] Vora, J., Patel, S., Sinha, S., Sharma, S., Srivastava, A., Chhabria, M., et al. Molecular docking, QSAR and ADMET based mining of natural compounds against prime targets of HIV. *J Biomol Struct Dyn*. 2019;
- [63] Zapadka, M., Kaczmarek, M., Kupcewicz, B., Dekowski, P., Walkowiak, A., Kokotkiewicz, A., et al. An application of QSRR approach and multiple linear regression method for lipophilicity assessment of flavonoids. *J Pharm Biomed Anal*. 2019;
- [64] Daina, A., Zoete, V. A BOILED-Egg To Predict Gastrointestinal Absorption and Brain Penetration of Small Molecules. *ChemMedChem*. 2016;
- [65] Singh, G., Satija, P., Singh, B., Sinha, S., Sehgal, R., Sahoo, S.C. Design, crystal structures and sustainable synthesis of family of antipyrine derivatives: Abolish to bacterial and parasitic infection. *J Mol Struct*. 2020;

*Corresponding author.

E-mail address: Emmanuel.marinho@ uece.br